

CHEMISTRY

A European Journal

A Journal of



Accepted Article

Title: Catalytic Intramolecular Cycloaddition Reactions Using a Discrete Molecular Architecture

Authors: Partha Sarathi Mukherjee, Bijan Roy, Anthonisamy Devaraj, Rupak Saha, Suprita Jharimune, and Ki-Whan Chi

This manuscript has been accepted after peer review and appears as an Accepted Article online prior to editing, proofing, and formal publication of the final Version of Record (VoR). This work is currently citable by using the Digital Object Identifier (DOI) given below. The VoR will be published online in Early View as soon as possible and may be different to this Accepted Article as a result of editing. Readers should obtain the VoR from the journal website shown below when it is published to ensure accuracy of information. The authors are responsible for the content of this Accepted Article.

To be cited as: *Chem. Eur. J.* 10.1002/chem.201702507

Link to VoR: <http://dx.doi.org/10.1002/chem.201702507>

Supported by
ACES

WILEY-VCH

FULL PAPER

Catalytic Intramolecular Cycloaddition Reactions Using a Discrete Molecular Architecture

Bijan Roy^a, Anthonisamy Devaraj^a, Rupak Saha^a, Suprita Jharimune^a, Ki-Whan Chi^b and Partha Sarathi Mukherjee^{a*}

Dedication ((optional))

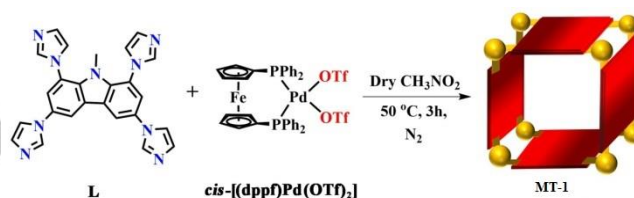
Abstract: A discrete tetragonal tube-shaped complex (**MT-1**) has been synthesized by coordination-driven self-assembly of a carbazole-based tetraimidazole donor **L** and a Pd(II) 90° acceptor, viz. $[cis-(dppf)Pd(OTf)_2]$ (dppf = diphenylphosphino ferrocene, OTf = $CF_3SO_3^-$). Complex **MT-1** was characterized by multinuclear NMR, ESI-MS and single crystal X-ray diffraction analysis (SCXRD), which showed its symmetrical tetrafacial tube-shaped architecture possessing a large cavity described by four aromatic walls. This coordination cage was successfully utilized as a molecular vessel to perform intramolecular cycloaddition reactions of O-allylated benzylidenebarbituric acid derivatives inside its confined nanospace. The presence of catalytic amount of **MT-1** promoted the [4+2] cycloaddition reactions in regio- and stereo-selective manner yielding the corresponding penta-/tetra-cyclouracil derivatives in good yields under mild reaction condition. This protocol is interesting compared to the literature reports for the synthesis of similar chromenopyran pyrimidinedione derivatives under high temperature reflux conditions or solid-state melt reaction (SSMR).

Introduction

Nature extensively exploits weak non-covalent interactions to modulate complex biochemical processes, which always remained a constant source of inspirations for the synthetic chemists.^[1] For example- enzymes, which are biological catalysts, generally contain a substrate binding site inside a hydrophobic cavity surrounded by the walls of protein molecules.^[2] An enzyme can specifically recognize and bind substrates, that get stabilized or activated by several weak non-covalent interactions that promote selective product formation and thus, creates ideal example of supramolecular catalysis. A supramolecular catalyst can modulate chemical reactions in several ways such as by (1) reducing entropy of the substrate(s); (2) stabilizing the transition state; (3) increasing effective concentration of the substrates; (4) spatial control over the specific product formation etc.^[3]

Synthetic chemists are constantly involved in designing molecular system which can efficiently emulate the enzymatic activity.^[4] A number of different types of container molecules with well-defined cavity have been reported so far including- crown ethers, cyclodextrins, cucurbituril, hydrogen bonded capsules, discrete metal-organic cages etc., which are proved to be efficient supramolecular catalysts.^[5]

Coordination-driven self-assembly has been evolved as one of the most successful methods to construct discrete molecular architectures with predesigned shapes, sizes and functionality owing to the strong directional nature of metal-ligand coordination and availability of plenty of organic donors of versatile geometries.^[6] In addition, the reversibility of certain metal-ligand bonds gives thermodynamic control over the self-assembly process which allows 'self-error correction' in order to form a desired architecture in high yield. Such architectures have been extensively explored for guest encapsulation, drug delivery, sensing, supramolecular catalysis etc.^[7] Coordination-driven self-assembly also provides opportunity to fine-tune the shape and property of the final architecture as well as the environment of the cavity by imparting changes in the building blocks in a way that does not alter the metal-ligand composition.



Scheme 1. Synthesis of the 'symmetrized' molecular tube **MT-1**.

In this article, we report the synthesis of a 'symmetrized' tetrafacial tube-shaped molecular architecture viz., **MT-1** by the self-assembly of a tetraimidazole donor **L** with a bulky Pd(II) 90° acceptor, i.e., $cis-[(dppf)Pd(OTf)_2]$ (dppf = 1,1'-diphenylphosphino ferrocene). **MT-1** was characterized by multinuclear (¹H and ³¹P) NMR spectroscopy, ESI-MS spectrometry and SCXRD analysis which showed **MT-1** to have tetrafacial tube-shaped architecture with symmetrical cavity, unlike our analogous water-soluble complex with less-symmetrical cavity, synthesized by using the same donor.^[8] The newly synthesized **MT-1** is soluble only in non-aqueous media. Most interestingly, **MT-1** is found to catalyze intramolecular hetero [4+2] cycloaddition reactions (IMHDA) of Benzylidenebarbituric acid derivatives (**1a-1f**) containing 1-Oxa-1,3-butadiene where the corresponding cyclized products (**2a-2f**) were obtained in good yields under relatively milder reaction condition in a stereo- and regio-controlled manner. The restriction of conformational

[a] Bijan Roy, Anthonisamy Devaraj, Rupak Saha, Suprita Jharimune and Prof. Partha Sarathi Mukherjee
Inorganic and Physical Chemistry Department
Indian Institute of Science
Bangalore-560012, India
E-mail: psm@ipc.iisc.ernet.in
FAX: 91-80-23601552

[b] Prof. Ki-Whan Chi
Department of Chemistry, University of Ulsan
Indian Institute of Science
Ulsan 680-749, Republic of Korea
Supporting information for this article is given via a link at the end of the document. ((Please delete this text if not appropriate))

FULL PAPER

flexibility of the substrates in the confined cavity of the cage leads to the product formation with increased selectivity, while similar kind of reactions need high temperature in absence of the cage and mostly yield mixture of isomers.^[9] While intermolecular [4+2] cycloaddition reactions in closed molecular cage are known, most of such reactions are stoichiometric and the products are trapped inside the cage. Larger windows in **MT-1** allow the products to come out and enabling the cycloaddition reactions in catalytic fashion.

Results and Discussion

The self-assembly was carried out in freshly distilled nitromethane under nitrogen atmosphere. When a colourless clear solution of **L** was added drop wise to a deep purple solution of the acceptor at room temperature, the sharp colour change into wine red indicated the product formation. The solution was heated at 50 °C for 3h, which was then completely dried and the residue was washed with chloroform and diethyl ether to obtain the desired product (**MT-1**) as brown powder. The ³¹P NMR spectrum of the compound in CD₃NO₂ showed the presence of two peaks of equal intensities at $\delta = 35.5$ and 34.2 ppm, which are significantly upfield shifted compared to the acceptor ($\delta = 46.2$ ppm) due to the enhanced Pd(II)-P back donation as a result of Pd(II)-**L** coordination (Figure 1).^[10] Such NMR pattern is expected for a molecular architecture bearing all the donor units in identical environment and considering the palladium ions are coordinated to two different sets of imidazole moieties in **L**.

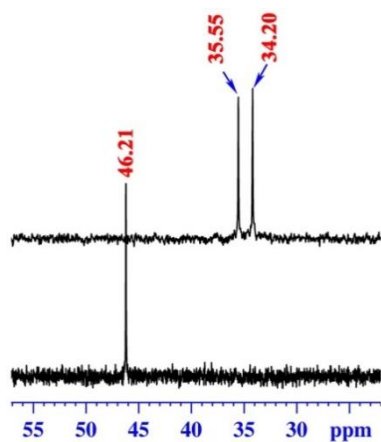


Figure 1: Comparison of ³¹P NMR spectra of **MT-1** recorded in CD₃NO₂ (up) and *cis*-[(dppf)Pd(OTf)₂] recorded in CDCl₃ (down).

Although the ¹H NMR spectra of the compound was very complex to interpret, the appearance of the sharp singlets of equal intensities corresponding to the cyclopentadienyl protons at $\delta = 5.30$ - 4.50 ppm region further suggested the formation of a pure product. Finally, the exact composition of the product was successfully determined from high resolution ESI-MS spectra obtained for the hexafluorophosphate analogue of **MT-1** (**MT-1**-PF₆), which was prepared by treating the compound with excess KPF₆ in methanol.^[11] The peaks obtained at $m/z = 2200.88$,

1733.50 and 1419.77 with clear isotopic distribution patterns corresponding to the 4+, 5+ and 6+ charged fragments

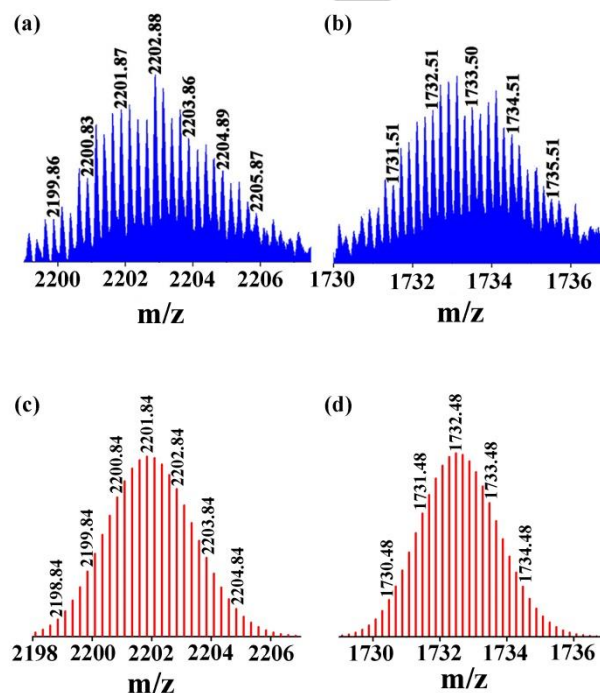
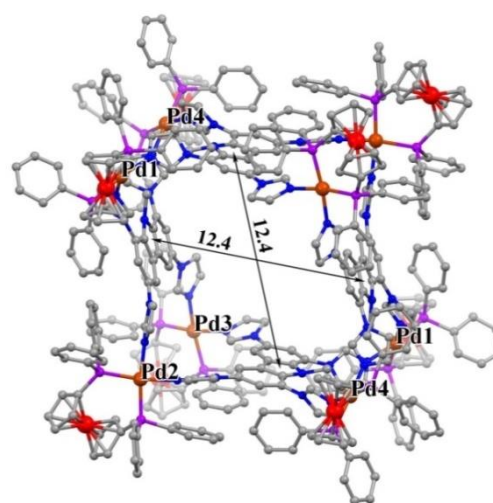


Figure 2: ESI-MS isotopic distribution patterns corresponding to the [**MT-1**-PF₆ - 4PF₆]⁴⁺ (calcd. $m/z = 2200.84$) (a) and [**MT-1**-PF₆ - 5PF₆]⁵⁺ (calcd. $m/z = 1733.47$) (b) charged species confirmed the formation of M₈L₄ assembly. (c) and (d) are the calculated isotopic distribution patterns for the 4+ and 5+ charged fragments, respectively.

of a M₈L₄ assembly are assigned for [**MT-1**-PF₆ - 4PF₆]⁴⁺ (calcd. $m/z = 2200.83$), [**MT-1**-PF₆ - 5PF₆]⁵⁺ (calcd. $m/z = 1733.47$) and [**MT-1**-PF₆ - 6PF₆]⁶⁺ (calcd. $m/z = 1419.73$) charged fragments, respectively (Figure 2).



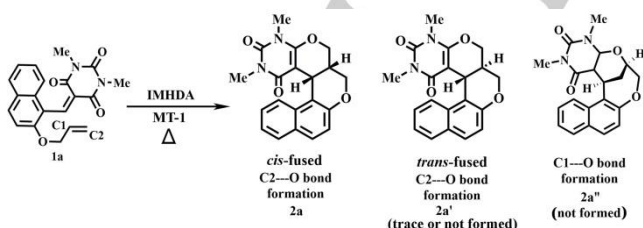
FULL PAPER

Figure 3: Ball and stick model representation of the crystal structure of **MT-1** showing distances between the opposite walls. Colour codes: Grey = C, blue = N, brown = Pd, red = Fe, and violet = P. H atoms are omitted for clarity.^[15]

Finally, the solid state structure of **MT-1** was unambiguously confirmed by SCXRD analysis.^[15] Suitable single crystals were grown by slow vapor diffusion of diisopropyl ether into a nitromethane solution of the complex. Brown rectangular crystals were very weakly diffracting and thus synchrotron radiation source was used for collecting X-ray data. The compound crystallized in monoclinic *C2/c* space group. Structure solution clearly showed **MT-1** to have a hollow tetrafacial tube architecture where the four donor moieties describe the walls of the tube and the Pd(II) ions are occupying the eight vertices. Moreover, the eight dppf groups are anchored outside the cavity (Figure 3). Interestingly, unlike the dissimilar spacing between the opposite donor walls in analogous water soluble tube,^[8] the gaps are equal in **MT-1** which measured to be ~12.4 Å. The adjacent Pd(II)-Pd(II) distances at the rhombus-shaped apertures are within 11.5-12.0 Å. Moreover, the tilt angle of all four *N*-Me groups are also identical (~29°), which again reflected the highly symmetric nature of the architecture. This further unveiled that, although the Pd1/Pd4 (similarly Pd2/Pd3, Figure 3) atoms form a crystallographically distinguishable pair, due to the overall symmetrical nature of the assembly their magnetic environments are same. Hence, the coordination of Pd1 and Pd4 with one set of imidazole moiety is responsible for a single peak in ³¹P NMR spectra. Similarly, the second peak is arising due to the coordination of Pd2 and Pd3 with the other set of imidazole in **L** (SI, Figure S3).

Formation of the symmetrical architecture of **MT-1** can be explained by the steric hindrance possessed by the bulky dppf groups. For a hypothetical non-symmetric tetrafacial tube structure of **MT-1**, the steric repulsion between the externally anchored phenyl groups of dppf moiety would be severe along the shorter walls of the tube, which is energetically not favorable. As a result, complex **MT-1** acquires symmetrical topology to distribute the steric strain 'homogenously' throughout the molecule. The versatile tunability of the donor angle in **L** as a result of the twisting of the imidazole moieties assisted the formation of symmetrical architecture.

Scheme 2: Intramolecular Hetero Diels-Alder Reaction of **1a**.



Hetero Diels-Alder reactions found prime significance in the synthesis of fused poly-heterocyclic compounds, which show promising bioactivity and are also used as intermediates in natural product synthesis.^[12] The intramolecular [4+2] cycloaddition of benzylidene derivatives obtained by the acid catalyzed Knoevenagel condensation of *O*-allylated salicylaldehydes and

barbituric acid provides a beautiful way to synthesize tetracyclic uracil compounds pertaining potential biological applications.^[13] Such reactions are usually performed at significantly higher temperatures (~150-200 °C) or in presence of toxic solvents like toluene, xylene etc. or via solid-state melt reaction (SSMR) technique, as mentioned in literature.^[13] Intramolecular hetero Diels-Alder reaction on benzylidene derivative (compound **1b**) was initially reported by Tietze^[13b] and co-workers employing xylene as solvent medium under reflux condition for 92 h which led to the formation of anticipated tetracyclic compound **2b** in good yield along with other isomer. Following this pioneering research Bhuyan^[14] and coworkers demonstrated an interesting protocol for accessing similar compound (**2b**) using benzylidene derivative (compound **1b**) in toluene under reflux condition for a period of 12 h which also led to the formation of **2b** along with other isomer which necessitates the development of new protocol for the stereo selective synthesis of such compound/s under mild reaction condition, while such stereo control can potentially be enabled by supramolecular catalysis using confined space.

Table 1: Optimization of Hetero Diels-Alder Reaction of **1a** Using **MT-1** as Molecular Vessel.

Entry	Loading (Mole %)	Temperature (°C)	Solvent	Yield (%)*	
				with cage	without cage
1	2.5	80	CH ₃ NO ₂	20	-----
2	5	80	CH ₃ NO ₂	34	-----
3	10	80	CH ₃ NO ₂	78	-----
4	20	80	CH ₃ NO ₂	81	-----
5	10	Rt	CH ₃ NO ₂	None	None
6	10	50	CH ₃ NO ₂	None	None
7	10	60	CH ₃ NO ₂	24	None
8	10	70	CH ₃ NO ₂	46	----
9	None	80	CH ₃ NO ₂	-----	11
10	10	80	CH ₃ CN	32	8

*Isolated by preparatory TLC. All the reactions were carried out for 48 h.

In order to check the suitability of the newly synthesized **MT-1** as molecular vessel for hetero Diels-Alder reaction, a few benzylidenebarbituric acid derivatives (**1a-1f**) were selected as substrates which consist of an 1-Oxa-1,3-butadiene as a heterodiene and a terminal alkene moiety as dienophile (Scheme 2 and Table 1). It was envisioned that upon encapsulation inside the large cavity of **MT-1**, the flexibility of the diene part of the

FULL PAPER

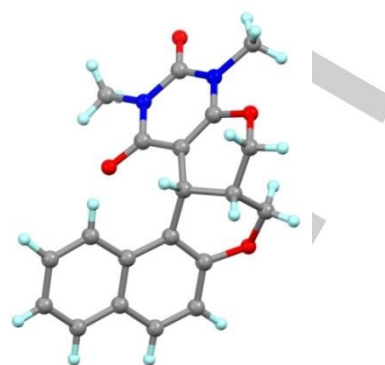
substrates will be restricted, which also may bring the diene closer to the dienophile to eventually facilitate the formation of [4+2] adduct in a regio- as well as stereo- controlled manner. The optimization of **MT-1** catalyzed IMHDA was performed using the naphthylidenebarbituric acid derivative (**1a**) as substrate (Scheme 2).

The requisite precursor *i.e.*, naphthylidenebarbituric acid derivative (**1a**) was prepared from 2-hydroxy-1-naphthaldehyde, allyl bromide and *N,N*-dimethylbarbituric acid through Williamson's ether synthesis followed by Knoevenagel condensation according to the procedure reported by Bhuyan and coworker.^[14] The condition for the **MT-1** catalytic cycloaddition reaction was optimized for **1a** at 80 °C for 48 h by using 10 mole percent catalyst loading which gave best result in nitromethane with an isolated yield of **2a** by 78% (Table 1). Interestingly, only 11% product was isolated when the same reaction was carried out in the absence of **MT-1**. The pentacyclic product (**2a**) was isolated by complete evaporation of the solvent followed by extraction with chloroform. The crude product was subsequently purified by preparative TLC and unambiguously characterized by ¹H, ¹³C NMR spectroscopy, ESI-MS spectrometry and elemental analysis.

The oxygen atom of the 1-Oxa-1,3-butadiene moiety of **1a** can attack either C₁ or C₂ atom of the terminal alkene group during the course of the cycloaddition (Scheme 2). While C₂ attack leads to the annulated product (*cis*-fused **2a** and *trans*-fused **2a'**), C₁ attack forms bridged heterocycle (**2a''**). We have observed predominantly the *cis*-fused product **2a** (based on the analysis of crude ¹H NMR spectra, SI, Figure S36) in good yield presumably due to the conformational restriction of the substrate by **MT-1** during cycloaddition whereas literature report is available for the significant formation of a mixture of products during IMHDA reaction which demonstrates the efficacy of the cage promoted cycloaddition.^[13b, 13c] In this direction we have also investigated the Diels-Alder reaction profile of **1a** in xylene under reflux condition over a period of 48 h which leads to the formation of mixture of isomers (SI, Figure S37) in accordance with the literature method.^[13b, 13c] The comparison of ¹H NMR spectrum of crude samples obtained by **MT-1** promoted cycloaddition (SI, Figure S36) as well as by the reported procedure without **MT-1** (SI, Figure S37) clearly demonstrates the stereo- as well as regio-selectivity of the cage promoted Diels-Alder reaction which is interesting in view of stereoselective organic transformations. One of the compounds in Table 2 (**2b**, entry 1) was reported earlier by Bhuyan^[14] in high yield (75%) along with other isomer under reflux condition in toluene. However, selectivity in stereo control by the confined cavity of **MT-1** (formation of *cis*-product), mild reaction condition and reusability of cage make the present protocol interesting. Moreover, the presence of the individual building blocks of **MT-1** [*i.e.* *cis*-(dppf)Pd(OTf)₂ and **L**] could not promote the cycloaddition reaction significantly, which indicates that the tetrafacial tube architecture plays key role in the stereo- and regio-selective product formation at relatively low temperature.

The regioselectivity and relative stereochemistry of the product are unambiguously confirmed by single crystal X-ray diffraction

Figure 4: Ball and stick model of the crystal structure of **2a**. Colour code: Grey=

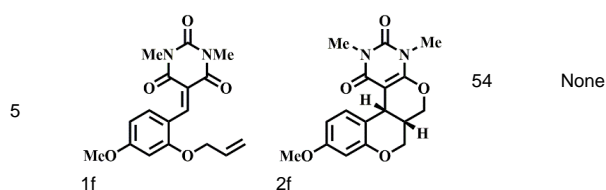


C, blue= N, red= O and cyan= H.^[15]

Table 2. Substrates and corresponding [4+2] cycloaddition products obtained by supramolecular catalysis with **MT-1**.*

Entry	Substrate	Product	Yield (%) With catalyst	Yield (%) Without catalyst
1			61	None
2			65	9
3			71	6
4			68	None

FULL PAPER



*Products were isolated by preparatory TLC. All the reactions were carried out for 48 h.

analysis^[15] (CCDC-1545091) which clearly shows that the product is **2a** which exhibited relative stereochemistry corresponding to the thermodynamically favorable *cis*-fused adduct (Figure 4). Interestingly, traditional intramolecular Diels-Alder reaction of the same substrate under high temperature in absence of the tube (**MT-1**) mostly yields a mixture of regio- and stereo-isomers. Thus the selective formation of **2a** promoted by the 'symmetrized' molecular tube (**MT-1**) is interesting in view of supramolecular catalysis as well as a molecular vessel for stereoselective organic transformation.

Unfortunately, the exact interaction between **MT-1** and the substrate **1a** could not be proved due to the fast equilibrium between the substrate in encapsulated and free forms in non-aqueous medium. Moreover, the strong absorption of the molecular tube in the visible wavelength region restricts the identification of the host-guest complex via UV-Vis spectroscopy. However, the successful encapsulation of **1a** by an analogous water soluble architecture^[8] in aqueous media was studied by UV-Vis (SI, Figure S32) and NMR (SI, Figure S33) spectroscopic techniques, which suggests that the cavity of **MT-1** is large enough to accommodate the substrates under investigation.

Furthermore, **MT-1** showed no sign of deformation upon heating up to 90 °C in presence of the substrate **1a** as observed from the variable temperature ³¹P NMR spectroscopy, confirming its thermal stability during the reaction (SI, Figure S34). A series of benzylidenebarbituric acid derivatives containing functionalized phenyl backbones (**1b-1f**) has been prepared and subsequently allowed to form Diels-Alder addition products under the similar reaction condition. In all the cases, the reactions smoothly led to the anticipated tetracyclic chromenopyran pyrimidinediones (**2b-**

f) in good yields and the results are summarized in Table 2.

The plausible mechanism for the tube catalysed intramolecular hetero Diels-Alder reaction is depicted in Figure 5. In homogeneous solution, the substrate molecule enters in to empty **MT-1** by collision and possibly gets stabilised via π -stacking interaction with the aromatic walls of the cavity. The confined space restricts the conformational flexibility of the substrate molecule and helps to orient the reacting functionalities, i.e. the diene and the dienophile in close proximity (S2 in Figure 5). At higher temperature, the substrate undergoes [4+2] cycloaddition to form the corresponding product (S3 in Figure 5). As the product has rigid non-planar tetra/pentacyclic structure (Figure 4), it hardly fits in to the cavity and eventually comes out to the bulk medium leaving the empty cage for further substrate encapsulation. The guest release is much easier from **MT-1** due to its wide rectangular aperture and good solubility of the products in organic medium. In contrast, the analogous water soluble architecture (**PSMBR-1**) could not catalyse the same cycloaddition reaction as the product does not come out in the aqueous medium due to the hydrophobicity. However, the kinetic study by ¹H NMR spectroscopy revealed that there is minute product inhibition taking place, which was evident from the decrease in the amount of the substrate conversion in presence of 10 mol% of the product at the beginning of the reaction (SI, Figure S41). This may be due to competition between the substrate and the product to get encapsulated inside the cavity of **MT-1**.

To judge the reusability of the molecular tube, the substrate **1a** was subjected to cycloaddition by using recovered **MT-1** from the reaction of the same substrate, which showed minute loss of efficiency in each step up to fifth cycle measured (SI, Figure S40). In addition, ³¹P NMR spectra of **MT-1** recovered after the fifth cycle of catalysis of **1a** showed no sign of disintegration (SI, Figure S36). This advocates the potency of **MT-1** as a supramolecular catalyst for such intramolecular reactions.

Scheme 3: Domino Reaction Catalyzed by Complex **MT-1**.

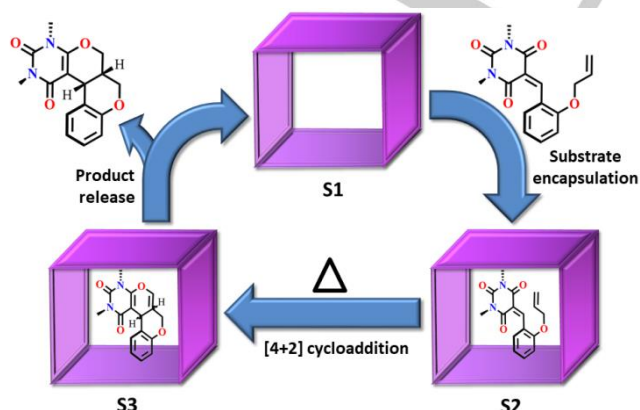
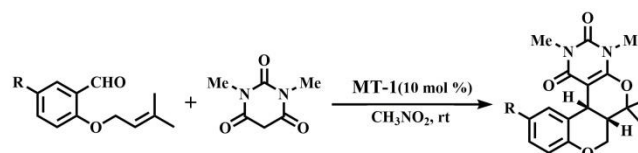


Figure 5: Pictorial representation showing the plausible mechanism of intramolecular hetero Diels-Alder reaction catalysed by **MT-1**. **S1** represents the empty molecular architecture **MT-1**.

	Product	Yield (%)**		Time (h)
		With 1	Without 1	
H (1g)	2g	73	None	22
Br (1h)	2h	71	None	22

**Isolation done by preparatory TLC

FULL PAPER

Domino reactions are very important in terms of atom economy, which involve consecutive steps where the functionality generated in the previous step undergoes reaction in the next step. Among various reactions, the domino Knoevenagel hetero Diels–Alder reaction is an efficient as well as convenient tool for accessing polyheterocyclic compounds and ranges of natural products. Construction of library of fused polyheterocyclic scaffolds has been performed using the domino Knoevenagel hetero Diels–Alder reaction as a key protocol.^[13d] In this aspect it occurs to us that the **MT-1** can be utilized as an efficient catalyst in domino reaction which will be very interesting in supramolecular catalysis using confined nanospace. In order to check the efficacy of the molecular tube (**MT-1**) to catalyze domino type synthesis of the tetracyclo uracil derivatives by starting from *O*-allylated salicylaldehydes, we prepared substrates (**1g-h**) containing dimethyl substituted terminal alkenes (activated). When treated with *N,N*-dimethylbarbituric acid in presence of 10 mol% of **MT-1** in nitromethane at room temperature for a period of 22 h, they successfully afforded the corresponding tetracyclo uracil derivatives in good yields, whereas, the same reactions in absence of the cage produced no detectable amount of products (Scheme 3) which successfully demonstrates the catalytic role of **MT-1** in domino Knoevenagel hetero Diels–Alder reaction representing the utility of supramolecular catalysis in domino reaction.

Conclusions

In conclusion, we have synthesized a new discrete tetrafacial molecular architecture (**MT-1**) by employing coordination-driven self-assembly of a *cis*-blocked Pd(II) 90° acceptor and the tetraimidazole donor **L**. The presence of large cavity with wide apertures makes complex **MT-1** a very potent molecular vessel for performing organic transformations. A series of *O*-allylated benzylidenebarbituric acid derivatives has been transformed in to the corresponding tetra/pentacyclo uracil products in presence of 10 mole% of **MT-1** under mild reaction condition. Interestingly, the similar reactions in absence of the tube resulted very less or no product formation, which successfully demonstrates the potency of the molecular vessel **MT-1** for enhanced conversion. While intermolecular [4+2] cycloaddition reactions in confined coordination cages are known, majority of such reactions are stoichiometric and products are generally trapped inside the cage. Catalytic nature of the reactions in the present case due to having larger open windows in our molecular tube makes our result important. The newly synthesized nanotube is quite efficient in controlling the regio- as well as stereo-selective pathways in the intramolecular hetero [4+2] cycloaddition reaction through the restriction of conformational flexibility of diene and tethered olefin. While literature reports mostly exemplify the formation of isomeric mixtures in such reactions, stereoselective transformation using **MT-1** as a molecular vessel is noteworthy. In addition, complex **MT-1** also promoted the Domino type synthesis of the tetracyclo product directly starting from the dimethyl substituted *O*-allylated salicylaldehyde derivatives at room temperature.

Experimental Section

Materials and Methods:

All the reagents and solvents were purchased from various commercial suppliers and used without further purification. NMR spectra were recorded in a Bruker 400 MHz spectrometer. UV-Visible and fluorescence spectra were recorded in Perkin Elmer Lambda-750 and Horiba Jobin fluoromax4 spectrophotometers, respectively. ESI-MS experiments were done in Agilent 6538 Ultra-High Definition (UHD) Accurate Mass Q-TOF spectrometer. Single crystal X-ray diffraction data for complex **MT-1** (CCDC-1545089) was collected in synchrotron beam line facility while the SCXRD data for **2a** was collected in a Bruker D8 QUEST CMOS diffractometer. The structures were solved by direct methods using SHELX-2013 incorporated in WinGX. Empirical absorption corrections were applied with SADABS. The non-hydrogen atoms of the main fragments were refined with anisotropic displacement coefficients. Hydrogen atoms were assigned with isotropic displacement coefficients, U(H) = 1.2U(C) or 1.5U (C-methyl), and their coordinates were allowed to ride on their respective carbons. Proper restraints were used to the minimum extent while solving the structure of **MT-1**. To further improve the structure solutions, final refinement was performed with the modification of the structure factors of the solvent molecules and counter anions using SQUEEZE option of PLATON.

Synthesis of MT-1. A 50 mL Schlenk flask was degassed and purged with nitrogen and then charged with 100 mg (0.10 mmol) of *cis*-[(dppf)Pd(OTf)₂] and 20 mL freshly distilled nitromethane. To the purple solution, a colourless solution of **L** (23.2 mg, 0.05 mmol) in 10 mL nitromethane was added very slowly by a syringe for 30 min with stirring. The solution finally became wine red which was then heated at 50 °C for 3 h. The solvent was evaporated completely under vacuum and the solid was washed with chloroform and diethyl ether and dried to obtain the product as dark red powder. Isolated yield: 110 mg (89%). ¹H NMR (400 MHz, CD₃NO₂): δ = 8.43, 8.26, 7.87, 7.83, 7.72, 7.54, 7.44, 7.37, 7.30, 7.23, 7.02, 6.29, 5.29, 5.13, 5.02, 4.89, 4.71, 4.65, 4.55, 2.11, 2.10. ³¹P NMR (CD₃NO₂): δ = 35.5, 34.2; Anal. Calcd. (%) for C₃₈₈H₃₀₀F₄₈Fe₈N₃₆O₄₈P₁₆S₁₆: C, 49.30; H, 3.20; N, 5.33. Found: C, 48.83; H, 3.55; N, 5.73. ESI-MS: *m/z* calcd for hexafluorophosphate analogue of **MT-1** (**MT-1**-PF₆) are 2200.84 for [**MT-1**-PF₆ - 4PF₆]⁴⁺, 1733.48 for [**MT-1**-PF₆ - 5PF₆]⁵⁺ and 1419.73 for [**MT-1**-PF₆ - 6PF₆]⁶⁺. Found: 2200.88, 1733.50 and 1419.77.

Synthesis of 1a: **1a** was synthesized in two steps following reported procedure.^[14] To a solution of 2-hydroxy-1-naphthaldehyde (344 mg, 2 mmol) in *N,N*-dimethylformamide (10 mL) was taken in a 50 mL round bottom flask and added with potassium carbonate (552 mg, 4 mmol). To this mixture, allyl bromide (0.9 mL, 10 mmol) was added slowly with constant stirring and the resultant solution was heated at 70 °C for 2 h. The reaction mixture was cooled down to room temperature and added with 80 mL of water. The solution was then extracted with chloroform. The organic layer was treated with sodium sulphate and the solvent was evaporated to get crude product which was purified by silica gel column chromatography (eluted with 20% diethyl ether in hexane) to get the intermediate 2-(allyloxy)-1-naphthaldehyde (**1a'**) as white solid. Yield: 400 mg (94%).

In the next step, **1a'** (400 mg, 1.88 mmol) was added slowly to a mixture of *N,N*-dimethyl barbituric acid (312 mg, 2 mmol) and aqueous HCl (25 mL, 13%), with constant stirring. After 3 h stirring at room temperature the precipitate was collected by filtration and washed with hot water and ethanol and dried under vacuum to get yellow coloured solid product in 89% overall yield (624 mg). ¹H NMR (400 MHz, CDCl₃): δ = 8.95 (s, 1H), 7.91-7.24 (m, 6H), 5.97 (d, 1H, *J* = 8 Hz), 5.38-5.23 (m, 2H), 4.69 (s, 2H), 3.46 (s, 3H), 3.25 (s, 3H). ¹³C NMR (100 MHz, CDCl₃): δ = 162.41, 160.11,

FULL PAPER

155.16, 153.47, 151.98, 133.37, 133.25, 132.19, 129.12, 128.94, 128.03, 124.75, 124.35, 121.82, 118.10, 118.06, 114.14, 70.30, 29.33, 28.73; ESI-MS *m/z*: Calculated $[M+H]^+$ = 351.1266; Found: 351.1356; Melting Point: 148 °C. Elemental analysis calcd (%) for (vacuum-dried) $C_{20}H_{18}N_2O_4$: C 68.56, H 5.18, N 8.00; found: C 68.59, H 4.98, N, 8.30.

Synthesis of 1b: **1b** was synthesized in a similar procedure as described for **1a** by using salicylaldehyde (244 mg, 2 mmol) as the starting material instead of 2-hydroxy-1-naphthaldehyde.^[14] The pure product was obtained as yellow solid in 92% overall yield (552 mg). ¹H NMR (400 MHz, $CDCl_3$): δ = 8.91 (s, 1H), 8.02 (d, 1H, *J* = 8Hz), 7.45 (t, 1H, *J* = 12Hz), 6.99 (t, 1H, *J* = 8Hz), 6.91 (d, 1H, *J* = 8Hz), 6.03-5.99 (m, 1H), 5.43-5.39 (m, 1H), 5.31-5.28 (m, 1H), 4.62 (d, 2H, *J* = 4Hz), 3.40 (s, 3H), 3.33 (s, 3H). ¹³C NMR (100 MHz, $CDCl_3$): δ = 163.0, 160.9, 159.1, 155.5, 152.0, 134.8, 133.2, 132.9, 122.9, 120.4, 118.4, 117.9, 112.2, 69.7, 29.4, 28.8; ESI-MS *m/z*: Calculated $[M+H]^+$ = 301.1110; Found: 301.1172; Melting Point: 150 °C. Elemental analysis calcd (%) for (vacuum-dried) $C_{16}H_{16}N_2O_4$: C 63.99, H 5.37, N 9.33; found: C 63.67, H 5.15, N 9.55.

Synthesis of 1c: The similar procedure was followed for the synthesis of **1c** by using 5-fluoro-2-hydroxybenzaldehyde (280 mg, 2 mmol) as the starting material. The pure product was obtained as yellow solid in 89% overall yield (566 mg). ¹H NMR (400 MHz, $CDCl_3$): δ = 8.82 (s, 1H), 7.84-7.80 (m, 1H), 7.15 (d, 1H, *J* = 4Hz), 6.86-6.83 (m, 1H), 6.02-6.00 (m, 1H), 5.42-5.28 (m, 2H), 4.59 (d, 2H, *J* = 4Hz), 3.40 (s, 3H), 3.33 (s, 3H); ¹³C NMR (100 MHz, $CDCl_3$): δ = 162.6, 160.7, 157.4, 155.3, 155.0, 153.7, 151.7, 132.7, 123.7, 121.1, 119.4, 119.1, 118.7, 118.5, 113.2, 113.1, 70.4, 29.4, 28.8; ESI-MS *m/z*: Calculated $[M+H]^+$ = 319.1015; Found: 319.1099; Melting Point: 109 °C.

Synthesis of 1d: **1d** was synthesized in similar manner as described above by using 5-bromo-2-hydroxybenzaldehyde (402 mg, 2 mmol). The product was obtained as yellow solid in 90% overall yield (682 mg). ¹H NMR (400 MHz, $CDCl_3$): δ = 8.75 (s, 1H), 8.12 (d, 1H, *J* = 4Hz), 7.54-7.51 (m, 1H), 6.80 (d, 1H, *J* = 8Hz), 5.99 (m, 1H), 5.42-5.29 (m, 1H), 4.60 (d, 2H, *J* = 4Hz), 3.41 (s, 3H), 3.34 (s, 3H); ¹³C NMR (100 MHz, $CDCl_3$): δ = 162.5, 160.5, 157.7, 153.4, 151.7, 136.7, 135.1, 132.5, 124.6, 119.0, 118.6, 113.8, 112.6, 70.0, 29.4, 28.9; ESI-MS *m/z*: Calculated $[M+H]^+$ = 379.0215; Found: 379.0296; Melting Point: 119 °C. Elemental analysis calcd (%) for (vacuum-dried) $C_{16}H_{15}BrN_2O_4$: C 50.68; H 3.99, N 7.39; found: C 50.49, H 4.02, N 7.55.

Synthesis of 1e: Same synthetic procedure was applied for the synthesis of **1e** using 2-hydroxy-3,5-diodobenzaldehyde (748 mg, 2 mmol). Pure product was obtained as yellow solid in 94% overall yield (1038 mg). ¹H NMR (400 MHz, $CDCl_3$): δ = 8.58 (s, 1H), 8.19 (s, 1H), 8.07 (s, 1H), 6.05 (s, 1H), 5.39-5.28 (m, 2H), 4.38 (s, 2H), 3.42 (s, 3H), 3.35 (s, 3H); ¹³C NMR (100 MHz, $CDCl_3$): δ = 161.7, 160.1, 158.6, 152.8, 151.5, 150.2, 140.5, 132.6, 130.5, 120.5, 119.9, 93.5, 88.03, 29.5, 29.0; ESI-MS *m/z*: Calculated $[M+H]^+$ = 552.9042; Found: 552.9168; Melting Point: 160 °C. Elemental analysis calcd (%) for (vacuum-dried) $C_{16}H_{14}I_2N_2O_4$: C 34.81, H 2.56, N 5.07; found: C 34.79, H 2.61, N 4.92.

Synthesis of 1f: Similar synthetic protocol starting with 2-hydroxy-4-methoxybenzaldehyde (304 mg, 2 mmol) provided **1f** as yellow solid in 85% yield (561 mg). ¹H NMR (400 MHz, $CDCl_3$): δ = 9.02 (s, 1H), 8.54 (d, 1H, *J* = 8Hz), 6.58-6.55 (m, 1H), 6.41 (s, 1H), 6.08-6.01 (m, 1H), 5.48-5.31 (m, 2H), 4.62 (d, 2H, *J* = 8Hz), 3.87 (s, 3H), 3.40 (s, 3H), 3.30 (s, 3H); ¹³C NMR (100 MHz, $CDCl_3$): δ = 163.76, 162.31, 161.54, 154.36, 136.43, 132.62, 118.62, 116.09, 114.39, 105.71, 99.05, 69.95, 56.16, 29.37, 28.79; ESI-MS *m/z*: Calculated $[M+H]^+$ = 331.1215; Found: 331.1294; Melting Point: 170 °C. Elemental analysis calcd (%) for (vacuum-dried) $C_{17}H_{18}N_2O_5$: C 61.81, H 5.49, N 8.48; found: C 61.43, H 5.33, N 8.49.

Procedure for the Catalytic Intramolecular Diels-Alder Reaction: To a clear solution of **MT-1** (37.7 mg, 0.004 mmol) in 4 mL nitromethane, the substrate (**1a-1f**, 0.04 mmol) was added and the solution was then heated at 80 °C for 48 h. After the completion of reaction as evidenced by TLC, the solvent was evaporated completely and the residue was extracted with chloroform. The crude products obtained after evaporation of chloroform were purified using preparative thin layer chromatography to afford pure samples.

Synthesis of 2a: By starting with **1a** (14 mg, 0.04 mmol), **2a** was obtained as off-white coloured solid in 78% yield (11 mg). ¹H NMR (400 MHz, $CDCl_3$): δ = 8.20 (d, 1H), 7.76 (d, 1H), 7.67 (d, 1H), 7.49 (t, 1H), 7.35 (t, 1H), 7.03 (d, 1H), 4.73 (d, 1H), 4.54 (s, 2H), 4.33 (s, 2H), 3.34 (s, 3H), 3.22 (s, 3H), 2.55 (m, 1H); ¹³C NMR (100 MHz, $CDCl_3$): δ = 162.8, 156.2, 151.7, 151.2, 134.8, 129.7, 129.6, 128.7, 126.2, 124.8, 123.7, 119.0, 116.8, 99.1, 69.6, 64.9, 31.8, 29.4, 28.7, 27.9; ESI-MS *m/z*: Calculated $[M+H]^+$ = 351.38; Found: 351.13. Elemental analysis calcd (%) for (vacuum-dried) $C_{20}H_{18}N_2O_4$: C 68.56, H 5.18, N 8.00; found: C 68.40, H 4.83, N 8.37.

Synthesis of 2b: **2b** was obtained as colourless solid in 61% yield (7.3 mg) by the Diels-Alder reaction of **2a** (12 mg, 0.04 mmol). ¹H NMR (400 MHz, $CDCl_3$): δ = 7.45-6.75 (m, 4H), 4.59-4.56 (m, 1H), 4.55-4.33 (m, 4H), 3.44 (s, 3H), 3.32 (s, 3H), 2.37-2.33 (m, 1H); ¹³C NMR (100 MHz, $CDCl_3$): δ = 164.6, 156.6, 152.2, 151.3, 131.0, 128.5, 124.1, 122.2, 117.2, 90.8, 68.3, 66.0, 30.1, 29.3, 29.1, 28.8; ESI-MS *m/z*: Calculated $[M+H]^+$ = 301.1110; Found: 301.1226; Melting point: 193 °C. Elemental analysis calcd (%) for (vacuum-dried) $C_{16}H_{16}N_2O_4$: C 63.99, H 5.37, N 9.33; found: C 63.65, H 5.12, N 9.09.

Synthesis of 2c: **2c** was obtained from **1c** (12.7 mg, 0.04 mmol) as off-white solid in 65% yield (8.3 mg). ¹H NMR (400 MHz, $CDCl_3$): δ = 7.23-7.20 (m, 1H), 6.81-6.78 (m, 1H), 6.72-6.69 (m, 1H), 4.58-4.55 (m, 1H), 4.36-4.25 (m, 4H), 3.43 (s, 3H), 3.33 (s, 3H), 2.35-2.32 (m, 1H); ¹³C NMR (100 MHz, $CDCl_3$): δ = 164.4, 159.2, 156.8, 151.2, 148.3, 125.3, 125.2, 118.1, 117.1, 116.9, 115.6, 115.4, 90.3, 68.3, 66.0, 29.9, 29.4, 29.3, 28.8; ESI-MS *m/z*: Calculated $[M+H]^+$ = 319.1015; Found: 319.1080; Melting point: 200 °C.

Synthesis of 2d: **2d** was formed as off-white solid in 71% yield (10.8 mg) by the Diels-Alder reaction of **1d** (15.2 mg, 0.04 mmol). ¹H NMR (400 MHz, $CDCl_3$): δ = 7.55-7.54 (m, 1H), 7.20 (d, 1H, *J* = 8Hz), 6.65 (d, 1H, *J* = 8Hz), 4.55-4.54 (m, 1H), 4.34-4.25 (m, 4H), 3.44 (s, 3H), 3.33 (s, 3H), 2.34 (t, 1H, *J* = 8Hz); ¹³C NMR (100 MHz, $CDCl_3$): δ = 164.3, 156.7, 151.4, 151.2, 133.5, 131.5, 126.2, 119.0, 114.2, 90.2, 68.2, 66.0, 29.8, 29.3, 29.1, 28.9; ESI-MS *m/z*: Calculated $[M+H]^+$ = 379.0215; Found: 379.0308; Melting point: 236 °C. Elemental analysis calcd (%) for (vacuum-dried) $C_{16}H_{15}BrN_2O_4$: C 50.68; H 3.99, N 7.39; found: C 51.00, H 3.79, N 7.46.

Synthesis of 2e: Similarly **2e** was obtained from **1e** (22.1 mg, 0.04 mmol) as off-white solid in 68% yield (15 mg). ¹H NMR (400 MHz, $CDCl_3$): δ = 7.88 (s, 1H), 7.68 (s, 1H), 4.58 (d, 1H, *J* = 8Hz), 4.47-4.16 (m, 5H), 3.42 (s, 3H), 3.33 (s, 3H), 2.36-2.33 (m, 1H); ¹³C NMR (100 MHz, $CDCl_3$): δ = 164.3, 156.8, 151.1, 145.8, 139.9, 127.0, 89.7, 86.5, 84.9, 68.0, 66.9, 29.8, 29.4, 29.3, 28.9; ESI-MS *m/z*: Calculated $[M+H]^+$ = 552.9042; Found: 552.9146; Melting point: 257 °C. Elemental analysis calcd (%) for (vacuum-dried) $C_{16}H_{14}I_2N_2O_4$: C 34.81, H 2.56, N 5.07; found: C 34.50, H 2.53, N 5.15.

Synthesis of 2f: Diels-Alder reaction of **1f** (13.2 mg, 0.04 mmol) formed **2f** in 54% yield (7.1 mg). ¹H NMR (400 MHz, $CDCl_3$): δ = 7.08 (d, 1H, *J* = 8Hz), 6.86-6.82 (m, 1H), 6.74 (d, 1H, *J* = 8Hz), 4.59 (d, 1H, *J* = 4Hz), 4.56-4.32 (m, 4H), 3.85 (s, 3H), 3.43 (s, 3H), 3.32 (s, 3H), 2.38-2.35 (m, 1H); ¹³C NMR (100 MHz, $CDCl_3$): δ = 164.5, 156.7, 151.3, 148.4, 141.7, 124.8,

FULL PAPER

122.47, 121.6, 110.0, 90.7, 68.3, 66.47, 56.3, 29.9, 29.3, 29.0, 28.8; ESI-MS m/z : Calculated $[M+H]^+$ = 331.1215; Found: 331.1300; Melting point: 238 °C. Elemental analysis calcd (%) for (vacuum-dried) $C_{17}H_{18}N_2O_5$: C 61.81, H 5.49, N 8.48; found: C 61.68, N 8.57.

Synthesis of 2g: 2-(3-methylbut-2-enyloxy)benzaldehyde (7.6 mg, 0.04 mmol) and N,N'-dimethyl barbutaric acid (6.24 mg, 0.04 mmol) were added with a solution of **MT-1** (37.7 mg, 0.004 mmol) in nitromethane and the mixture was stirred at room temperature for 22 h. After the completion of reaction the solvent was evaporated completely and the residue was extracted with chloroform. The crude product obtained upon evaporation of the solvent was purified by preparative thin layer chromatography to provide **2g** in 73% yield (9.59 mg). 1H NMR (400 MHz, $CDCl_3$): δ = 7.42 (d, 1H, J = 8Hz), 7.10-6.69 (m, 3H), 4.48-4.34 (m, 3H), 3.42 (s, 3H), 3.34 (s, 3H), 2.15-2.14 (m, 1H), 1.63 (s, 3H), 1.23 (s, 3H); ^{13}C NMR (100 MHz, $CDCl_3$): δ = 155.9, 153.9, 151.6, 130.2, 128.3, 123.3, 121.6, 116.2, 89.0, 84.4, 65.2, 39.2, 29.4, 29.3, 28.6, 24.3; ESI-MS m/z : Calculated $[M+H]^+$ = 329.1423; Found: 329.1494; Melting point: 205 °C. Elemental analysis calcd (%) for (vacuum-dried) $C_{18}H_{20}N_2O_4$: C 65.84, H 6.14, N 8.53; found: C 65.91, H 6.05, N 8.71.

Synthesis of 2h: **2h** was obtained by following the same protocol as applied for **2g** starting with 5-bromo-2-(3-methylbut-2-enyloxy)benzaldehyde (8.04 mg, 0.04 mmol) and N,N'-dimethyl barbutaric acid (6.24 mg, 0.04 mmol) and the product was obtained in 71% yield (11.6 mg). 1H NMR (400 MHz, $CDCl_3$): δ = 7.55 (d, 1H, J = 4Hz), 7.19-7.16 (m, 1H), 6.69 (d, 1H, J = 8Hz), 4.42-4.40 (m, 2H), 4.31 (d, 1H, J = 8Hz), 3.43 (s, 3H), 3.34 (s, 3H), 2.13 (d, 1H, J = 4Hz), 1.61 (s, 3H), 1.21 (s, 3H); ^{13}C NMR (100 MHz, $CDCl_3$): δ = 164.3, 156.0, 153.1, 151.5, 132.79, 131.3, 125.6, 118.1, 113.8, 88.4, 84.3, 65.3, 38.9, 29.4, 29.3, 28.6, 24.2; ESI-MS m/z : Calculated $[M+H]^+$ = 407.0528; Found: 407.0618; Melting point: 200 °C. Elemental analysis calcd (%) for (vacuum-dried) $C_{18}H_{19}BrN_2O_4$: C 53.08; H 4.70, N 6.88; found: C 53.28, H 4.77, N 7.03.

Acknowledgements

P.S.M. thanks the Science and Engineering Research Board (New Delhi) for research grant [Grant No. EMR/2015/002353]. A.D. is grateful to UGC (New Delhi) for the Dr. D. S. Kothari postdoctoral fellowship. X-ray diffraction experiments using the synchrotron radiation for complex **MT-1** were performed at the Pohang Accelerator Laboratory in Korea.

Keywords: Supramolecular chemistry • self-assembly • cage compounds • catalysis • coordination chemistry

[1](a)S. Sivakova, S. J. Rowan, *Chem. Soc. Rev.* **2005**, *34*, 9-21; (b)D. Philp, J. F. Stoddart, *Angew. Chem. Int. Ed.* **1996**, *35*, 1154-1196; (c)J. M. Zayed, N. Nouvel, U. Rauwald, O. A. Scherman, *Chem. Soc. Rev.* **2010**, *39*, 2806-2816; (d)C. K. McLaughlin, G. D. Hamblin, H. F. Sleiman, *Chem. Soc. Rev.* **2011**, *40*, 5647-5656; (e)G. M. Whitesides, B. Grzybowski, *Science* **2002**, *295*, 2418-2421; (f)B. Philip, *Nanotechnology* **2002**, *13*, R15; (g)J.-M. Lehn, *Proc. Natl. Acad. Sci. U.S.A.* **2002**, *99*, 4763-4768; (h)N. C. Gianneschi, M. S. Masar, C. A. Mirkin, *Acc. Chem. Res.* **2005**, *38*, 825-837; (i)Y. Ueda, H. Ito, D. Fujita, M. Fujita, *J. Am. Chem. Soc.* **2017**.

[2](a)T. L. Poulos, B. C. Finzel, A. J. Howard, *J. Mol. Biol.* **1987**, *195*, 687-700; (b)M. F. Perutz, M. G. Rossmann, A. F. Cullis, H. Muirhead, G. Will, A. C. T. North, *Nature* **1960**, *185*, 416-422; (c)T. L. Poulos, *Chem. Rev.* **2014**, *114*, 3919-3962; (d)F. Berkovitch, Y. Nicolet, J. T. Wan, J. T. Jarrett, C. L. Drennan, *Science* **2004**, *303*, 76-79; (e)T. V. Vendelboe, P. Harris, Y. Zhao, T. S. Walter, K. Harlos, K. El Omari, H. E. M. Christensen, *Sci. Adv.* **2016**, *2*.

[3](a)J. Kang, J. Rebek, *Nature* **1996**, *382*, 239-241; (b)J. Liu, L. Chen, H. Cui, J. Zhang, L. Zhang, C.-Y. Su, *Chem. Soc. Rev.* **2014**, *43*, 6011-6061; (c)M. Raynal, P. Ballester, A. Vidal-Ferran, P. W. N. M. van Leeuwen, *Chem. Soc. Rev.* **2014**, *43*, 1660-1733; (d)M. Raynal, P. Ballester, A. Vidal-Ferran, P. W. N. M. van Leeuwen, *Chem. Soc. Rev.* **2014**, *43*, 1734-1787; (e)F. Ortega-Caballero, C. Rousseau, B. Christensen, T. E. Petersen, M. Bols, *J. Am. Chem. Soc.* **2005**, *127*, 3238-3239; (f)K. Surendra, N. S. Krishnaveni, A. Mahesh, K. R. Rao, *J. Org. Chem.* **2006**, *71*, 2532-2534; (g)V. Kunz, M. Schulze, D. Schmidt, F. Würthner, *ACS Energy Lett.* **2017**, *2*, 288-293; (h)L. Guy, J.-P. Dutasta, A. Martinez, in *Effects of Nanoconfinement on Catalysis* (Ed.: R. Poli), Springer International Publishing, Cham, **2017**, pp. 1-15; (i)J. Meeuwissen, J. N. H. Reek, *Nat. Chem.* **2010**, *2*, 615-621; (j)M. D. Pluth, R. G. Bergman, K. N. Raymond, *Acc. Chem. Res.* **2009**, *42*, 1650-1659; (k)M. D. Levin, D. M. Kaphan, C. M. Hong, R. G. Bergman, K. N. Raymond, F. D. Toste, *J. Am. Chem. Soc.* **2016**, *138*, 9682-9693; (l)D. M. Kaphan, M. D. Levin, R. G. Bergman, K. N. Raymond, F. D. Toste, *Science* **2015**, *350*, 1235-1238. (m) S. H. A. M. Leenders, R. Gramage-Doria, B. de Bruin, J. N. H. Reek *Chem. Soc. Rev.*, **2015**, *44*, 433-448. (n) C. J. Brown, F. D. Toste, R. G. Bergman, K. N. Raymond, *Chem. Rev.*, **2015**, *115*, 3012-3035. (o) J. H. Jordan, B. C. Gibb, *Chem. Soc. Rev.*, **2015**, *44*, 547-585. (p) L. Catti, Q. Zhang, K. Tiefenbacher, *Chem. Eur. J.*, **2016**, *22*, 9060-9066.

[4](a)J. Yano, V. Yachandra, in *XAFS Techniques for Catalysts, Nanomaterials, and Surfaces* (Eds.: Y. Iwasawa, K. Asakura, M. Tada), Springer International Publishing, Cham, **2017**, pp. 451-465; (b)Y. Tu, F. Peng, A. Adawy, Y. Men, L. K. E. A. Abdelmohsen, D. A. Wilson, *Chem. Rev.* **2016**, *116*, 2023-2078; (c)N. Le Poul, Y. Le Mest, I. Jabin, O. Reinaud, *Acc. Chem. Res.* **2015**, *48*, 2097-2106; (d)S. Chatterjee, K. Sengupta, S. Hematian, K. D. Karlin, A. Dey, *J. Am. Chem. Soc.* **2015**, *137*, 12897-12905; (e)T. C. Brunold, *Proc. Natl. Acad. Sci. U.S.A.* **2007**, *104*, 20641-20642.

[5](a)T. M. Bräuer, Q. Zhang, K. Tiefenbacher, *Angew. Chem. Int. Ed.* **2016**, *55*, 7698-7701; (b)Q. Zhang, L. Catti, V. R. I. Kaila, K. Tiefenbacher, *Chem. Sci.* **2017**, *8*, 1653-1657; (c)Y. Qiao, L. Zhang, J. Li, W. Lin, Z. Wang, *Angew. Chem. Rev.* **2016**, *128*, 12970-12974; (d)P. Ballester, M. Fujita, J. Rebek, *Chem. Soc. Rev.* **2015**, *44*, 392-393; (e)R. Kulasekharan, R. Choudhury, R. Prabhakar, V. Ramamurthy, *Chem. Commun.* **2011**, *47*, 2841-2843; (f)Z. Qi, T. Heinrich, S. Moorthy, C. A. Schalley, *Chem. Soc. Rev.* **2015**, *44*, 515-531; (g)P. Howlander, P. Das, E. Zangrando, P. S. Mukherjee, *J. Am. Chem. Soc.* **2016**, *138*, 1668-1676; (h)D. Samanta, S. Mukherjee, Y. P. Patil, P. S. Mukherjee, *Chem. Eur. J.* **2012**, *18*, 12322-12329; (i)W. Wang, Y.-X. Wang, H.-B. Yang, *Chem. Soc. Rev.* **2016**, *45*, 2656-2693; (j)M. Yoshizawa, J. K. Klosterman, M. Fujita, *Angew. Chem. Int. Ed.* **2009**, *48*, 3418-3438; (k)C. J. Hastings, M. P. Backlund, R. G. Bergman, K. N. Raymond, *Angew. Chem. Int. Ed.* **2011**, *50*, 10570-10573.

[6](a)S. M. Jansze, M. D. Wise, A. V. Vologzhanina, R. Scopelliti, K. Severin, *Chem. Sci.* **2017**; (b)M. Fujita, M. Tominaga, A. Hori, B. Therrien, *Acc. Chem. Res.* **2005**, *38*, 369-378; (c)R. Chakrabarty, P. S. Mukherjee, P. J. Stang, *Chem. Rev.* **2011**, *111*, 6810-6918; (d)X. Yan, T. R. Cook, J. B. Pollock, P. Wei, Y. Zhang, Y. Yu, F. H., P. J. Stang, *J. Am. Chem. Soc.* **2014**, *136*, 4460-4463; (e)G. Yu, T. R. Cook, Y. Li, X. Yan, D. Wu, L. Shao, J. Shen, G. Tang, F. Huang, X. Chen, P. J. Stang, *Proc. Natl. Acad. Sci. U.S.A.* **2016**, *113*, 13720-13725.

[7](a)M. J. Wiester, P. A. Ulmann, C. A. Mirkin, *Angew. Chem. Int. Ed.* **2011**, *50*, 114-137; (b)H. Vardhan, M. Yusubov, F. Verpoort, *Coord. Chem. Rev.* **2016**, *306*, Part 1, 171-194; (c)Y.-R. Zheng, K. Suntharalingam, T. C. Johnstone, S. J. Lippard, *Chem. Sci.* **2015**, *6*, 1189-1193; (d)F. Schmitt, J. Freudenreich, N. P. E. Barry, L. Juillerat-Jeanneret, G. Süß-Fink, B. Therrien, *J. Am. Chem. Soc.* **2012**, *134*, 754-757; (e)N. Ahmad, H. A. Younus, A. H. Chughtal, F. Verpoort, *Chem. Soc. Rev.* **2015**, *44*, 9-25; (f)S. M. McNeill, D. Preston, J. E. M. Lewis, A. Robert, K. Knerr-Rupp, D. O. Graham, J. R. Wright, G. I. Giles, J. D. Crowley, *Dalton Trans.* **2015**, *44*, 11129-11136; (g)A. Ahmedova, R. Mihaylova, D. Momekova, P. Shestakova, S. Stoykova, J. Zaharieva, M. Yamashina, G. Momekov, M. Akita, M. Yoshizawa, *Dalton Trans.* **2016**, *45*, 13214-13221; (h)N. Singh, S. Jang, J.-H. Jo, D. H. Kim, D. W. Park, I. Kim, H. Kim, S. C. Kang, K.-W. Chi, *Chem. Eur. J.* **2016**, *22*, 16157-16164; (i)M. L. Saha, X. Yan, P. J. Stang, *Acc. Chem. Res.* **2016**, *49*, 2527-2539; (j)S. Shanmugaraju, P. S. Mukherjee, *Chem. Eur. J.* **2015**, *21*, 6656-6666; (k)W. M. Bloch, Y. Abe, J. J. Holstein, C. M. Wandtke, B. Dittrich, G. H. Clever, *J. Am. Chem. Soc.* **2016**, *138*, 13750-13755; (l)N. Mittal, M. L. Saha, M. Schmittel, *Chem. Commun.* **2016**, *52*, 8749-8752; (m)M. L. Saha, M. Schmittel, *Inorg. Chem.* **2016**, *55*, 12366-12375; (n)C. A. Wiley, L. R. Holloway, T. F. Miller, Y. Lyon, R. R. Julian, R. J. Hooley, *Inorg. Chem.* **2016**, *55*, 9805-9815; (o)L. R. Holloway, M. C. Young, G. J. O. Beran, R. J. Hooley, *Chem. Sci.* **2015**, *6*, 4801-4806; (p)S. Karthikeyan, V. Ramamurthy, *J. Org. Chem.* **2007**, *72*, 452-458.

[8]B. Roy, A. K. Ghosh, S. Srivastava, P. D'Silva, P. S. Mukherjee, *J. Am. Chem. Soc.* **2015**, *137*, 11916-11919.

FULL PAPER

- [9](a)C. García-Simón, R. Gramage-Doria, S. Raoufmoghaddam, T. Parella, M. Costas, X. Ribas, J. N. H. Reek, *J. Am. Chem. Soc.* **2015**, *137*, 2680-2687; (b)M. V. S. N. Maddipatla, L. S. Kaanumalle, A. Natarajan, M. Pattabiraman, V. Ramamurthy, *Langmuir* **2007**, *23*, 7545-7554.
- [10](a)B. Jiang, J. Zhang, J.-Q. Ma, W. Zheng, L.-J. Chen, B. Sun, C. Li, B.-W. Hu, H. Tan, X. Li, H.-B. Yang, *J. Am. Chem. Soc.* **2016**, *138*, 738-741; (b)Z. Zhou, X. Yan, M. L. Saha, M. Zhang, M. Wang, X. Li, P. J. Stang, *J. Am. Chem. Soc.* **2016**, *138*, 13131-13134; (c)S. Shanmugaraju, A. K. Bar, H. Jadhav, D. Moon, P. S. Mukherjee, *Dalton Trans.* **2013**, *42*, 2998-3008.
- [11](a)B. Roy, E. Zangrando, P. S. Mukherjee, *Chem. Commun.* **2016**, *52*, 4489-4492; (b)X. Yan, M. Wang, T. R. Cook, M. Zhang, M. L. Saha, Z. Zhou, X. Li, F. Huang, P. J. Stang, *J. Am. Chem. Soc.* **2016**, *138*, 4580-4588.
- [12](a)K. C. Nicolaou, S. A. Snyder, T. Montagnon, G. Vassilikogiannakis, *Angew. Chem. Int. Ed.* **2002**, *41*, 1668-1698; (b)B. S. Bodnar, M. J. Miller, *Angew. Chem. Int. Ed.* **2011**, *50*, 5630-5647; (c)M. Toyota, C. Komori, M. Ihara, *J. Org. Chem.* **2000**, *65*, 7110-7113; (d)V. Eschenbrenner-Lux, K. Kumar, H. Waldmann, *Angew. Chem. Int. Ed.* **2014**, *53*, 11146-11157.
- [13](a)L. F. Tietze, *J. Heterocycl. Chem.* **1990**, *27*, 47-69; (b)M. Buback, K. Gerke, C. Ott, L. F. Tietze, *Chem. Ber.* **1994**, *127*, 2241-2248; (c)L. F. Tietze, T. Brumby, M. Pretor, G. Remberg, *J. Org. Chem.* **1988**, *53*, 810-820; (d) L. F. Tietze, *Chem. Rev.* **1996**, *96*, 115-136.
- [14] I. Devi, P. J. Bhuyan, *Tetrahedron Lett.* **2004**, *45*, 7727-7728.
- [15]Structure of **MT-1** and **2a** were clearly confirmed by single-crystal X-ray data. CCDC-1545089 [for **MT-1**] and CCDC-1545091 (for **2a**) contain the crystallographic data.

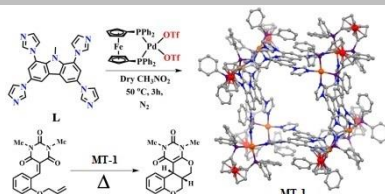
FULL PAPER

Entry for the Table of Contents (Please choose one layout)

Layout 1:

FULL PAPER

A discrete tetragonal tube-shaped molecular architecture (**MT-1**) has been synthesized by self-assembly of a tetraimidazole donor **L** and a Pd(II) 90° acceptor. Complex **MT-1** was utilized as a molecular vessel to perform intramolecular hetero Diels-Alder reactions of *O*-allylated benzylidenebarbuturic acid derivatives inside its confined nanospace. The presence of catalytic amount of the molecular tube promoted the [4+2] cycloaddition reactions in highly regio- and stereo-selective manner yielding the corresponding penta / tetracyclouracil derivatives in good yields under mild reaction condition.



Bijan Roy^a, Anthonisamy Devaraj^a,
Rupak Saha^a, Suprita Jharimune^a, Ki-
Whan Chi^b and Partha Sarathi
Mukherjee^{a*}

Page No. – Page No.

Catalytic Intramolecular
Cycloaddition Reactions Using a
Discrete Molecular Architecture

Layout 2:

FULL PAPER

((Insert TOC Graphic here; max. width: 11.5 cm; max. height: 2.5 cm))

Text for Table of Contents

Author(s), Corresponding Author(s)*

Page No. – Page No.

Title